

Itinerant and localized magnetism on the triangular lattice: sodium rich phases of Na_xCoO_2

Meng Gao, Sen Zhou, and Ziqiang Wang

Department of Physics, Boston College, Chestnut Hill, MA 02467

(Dated: August 12, 2021)

We study the interplay between correlation, itinerant ferromagnetism and local moment formation on the electron doped triangular lattice of sodium cobaltates Na_xCoO_2 . We find that strong correlation renormalizes the Stoner criterion and stabilizes the paramagnetic state for $x < x_c \simeq 0.67$. For $x > x_c$, ferromagnetic (FM) order emerges. The enhanced Na dopant potential fluctuations play a crucial role in the sodium rich phases and lead to an inhomogeneous FM state, exhibiting nonmagnetic Co^{3+} patches, antiferromagnetic (AF) correlated regions, and FM clusters with AF domains. Hole doping the band insulator at $x=1$ leads to the formation of local moments near the Na vacancies and AF correlated magnetic clusters. We explain recent observations by neutron, μSR , and NMR experiments on the evolution of the magnetic properties in the sodium rich phases.

PACS numbers: 74.25.Ha, 71.27.+a, 75.20.Hr

Sodium cobaltates, Na_xCoO_2 , are electron doped transition metal oxides with a layered, hexagonal lattice structure. The Co^{4+} has a $3d^9$ configuration with 5 d-electrons occupying the three lower t_{2g} orbitals. At a Na density x , the average Co valence is $\text{Co}^{(4-x)}$, evolving from an open shell Co^{4+} with low-spin state $S = 1/2$ at $x = 0$ to a closed shell Co^{3+} with a low-spin state $S = 0$ at $x = 1$. The cobaltates provide an almost ideal low-spin lattice fermion system for studying the physics of correlation and geometrical frustration in the charge, spin, and orbital sectors.

Since the discovery of unconventional superconductivity near $x = 0.3$ upon water-intercalation in this material [1], a broad spectrum of experiments have been performed, yielding a rich and complex phase diagram with many unexpected and novel properties. Magnetism plays an essential role in the sodium rich region with $x > 0.5$. The metallic transport coexists with a Curie-Weiss magnetic susceptibility leading to a novel ‘‘Curie-Weiss metal’’ [2]. Neutron scattering and NMR experiments find strong in-plane ferromagnetic (FM) fluctuations at high temperatures and magnetically ordered states emerge for $x > 0.75$ [3]. At $x = 0.82$, neutron scattering determined that in-plane FM order and inter-layer antiferromagnetic (AF) order develops below a 3D Neel temperature $T_N = 20\text{K}$ [4]. There is increasing experimental evidence for unexpected strong correlation effects as the cobaltates approach the band insulating limit at $x = 1$. Recent μSR experiments discovered the emergence of AF correlated magnetic clusters and localized magnetic moments for $x > 0.96$ [5]. Interestingly, the high thermoelectric power of the sodium cobaltate is found in the sodium rich region which is likely to have a related magnetic origin [6]. The nature of the magnetism in the sodium rich region has been the focus of several theoretical work [7, 8, 9, 10].

In this paper, we study the magnetic properties, both itinerant and localized, of strongly correlated electrons on

the triangular lattice, and present a theoretical description of the novel magnetism observed by experiments in the sodium rich phases. Strong correlation plays an important role in the electronic structure of the cobaltates. It has been shown recently [11, 12, 13, 14] that correlation-induced corrections to the crystal field splitting and bandwidths of the LDA calculations [15] can produce a single renormalized band of mostly a_{1g} character at the Fermi level as observed by angle resolved photoemission (ARPES) [16, 17, 18, 19]. Here we show that the description of the magnetism in the cobaltates, too, requires a proper account of the large Coulomb repulsion U at the cobaltate sites. Indeed, in the LSDA+ U theory [20], which accounts for the correlation effects in the Hartree-Fock approach, the LDA paramagnetic (PM) state is always unstable and the ground state is a fully polarized ferromagnet at all doping for U as small as 2eV . This disagrees with experiments that the in-plane FM order does not emerge until $x > 0.75$ and that a single spin-degenerate Fermi surface of the Luttinger area is observed by ARPES for $x < 0.72$ [18]. We show that the weak-coupling Stoner instability is unphysical when correlation is strong. Using a strong-coupling Gutzwiller projection approach, we show that the Stoner criterion is strongly renormalized and the spin dependent self-energy scales with the average kinetic energy instead of U . The PM phase is in fact stable against itinerant FM below a critical electron doping $x_c \simeq 0.67$ above which in-plane FM order emerges.

In the sodium-rich region, we show that the enhanced electrostatic potential fluctuations due to the disordered Na dopants lead to the coexistence of localized and itinerant electronic states with inhomogeneous FM order, exhibiting nonmagnetic Co^{3+} patches, AF correlated local regions, and FM clusters with AF domain walls. For very high Na doping, the dilute Na vacancies enhance the strong correlation effects by increasing the localization tendency of the carriers [21]. We consider the case of

a few holes (Na vacancies) doped into the band insulator at $x = 1$, and find that the hidden correlation effects are brought out upon the slightest amount of doping. Specifically, a single hole/Na vacancy induces an $S = 1/2$ local moment. We address the interactions between the local moments and the evolution into magnetic clusters and eventually to the macroscopic FM ordered state with decreasing Na doping and provide a theoretical description of neutron [4], μ SR [5] and NMR experiments [22].

We start with the Hubbard model for the relevant low-energy quasiparticle band of approximate a_{1g} character,

$$H = \sum_{i,j,\sigma} t_{ij} c_{i\sigma}^\dagger c_{j\sigma} + \sum_i U \hat{n}_{i\uparrow} \hat{n}_{i\downarrow}, \quad (1)$$

where $c_{i\sigma}^\dagger$ creates a *hole* and U (~ 5 eV for the cobaltates [16]) is the on-site Coulomb repulsion. To model the a_{1g} band, we consider up to 3rd nearest-neighbor hopping $(t_1, t_2, t_3) = (-0.202, 0.035, 0.029)$ eV [23]. The hole density $n_i = n_{i\uparrow} + n_{i\downarrow} = 1 - x_i$ with x_i the electron doping, is fixed by the chemical potential μ . Due to the small direct Co-Co overlap and the large U and the 90° O-Co-O bond angle, the AF superexchange J in the cobaltates is small [24], consistent with the value $J \sim 5$ meV determined by inelastic neutron scattering [4]. We thus focus on the in-plane magnetism of the kinetic origin. To study the 3D magnetic ordering transition at finite temperature, a small interlayer exchange coupling is needed.

In the weak-coupling HF theory, itinerant FM is due to the Stoner instability, i.e. the divergence of the uniform susceptibility $\chi = \chi_0 / (1 - UN_F/2)$, where χ_0 is the free-electron value and N_F is the DOS at the Fermi level. The large DOS of the cobaltates would lead to FM order for all x for U greater than a value less than 2eV [20], clearly inconsistent with experiments. The failure of the HF or LSDA+U theory lies in the spin-dependent self-energy correction that scales with U . This is unphysical for U larger than the bandwidth. For example, for large U , the system can simply avoid paying the energy penalty for double occupation in Eq. (1) by reverting to a fully spin-polarized state that involves only the kinetic energy. This is the physics behind the Nagaoka theorem: on square lattices, the ground state of the infinite- U Hubbard model doped with a single hole is a fully polarized FM. At finite hole density, the Nagaoka state is lower in energy than the Gutzwiller projected PM state at low doping [26]. Interestingly, on the triangular lattice the kinetic energy is frustrated in the sense that hopping around an elemental triangle picks up a negative sign, the Nagaoka state is not the ground state for a single hole [27]. To study FM at finite electron doping, we consider the large- U limit captured by the projection of double occupation. To make analytical progress, we treat the latter by Gutzwiller approximation (GA) in the grand canonical ensemble where the projected wave function

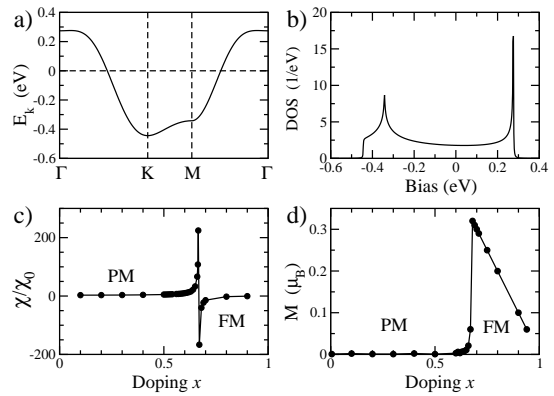


FIG. 1: Renormalized a_{1g} quasiparticle dispersion (a) and the DOS (b) in the PM state at $x=0.3$. (c) The uniform susceptibility showing the renormalized Stoner instability at $x_c \simeq 0.67$. (d) The magnetization phase diagram.

can be written as

$$|\Psi\rangle = \prod_i y_{i\uparrow}^{\hat{n}_{i\uparrow}} y_{i\downarrow}^{\hat{n}_{i\downarrow}} (1 - \hat{n}_{i\uparrow} \hat{n}_{i\downarrow}) |\Psi_0\rangle. \quad (2)$$

Here Ψ_0 is an unprojected Slater determinant state and $y_{i\sigma}$ is a spin-dependent local fugacity that maintains the equilibrium and the local densities upon projection. The GA is then equivalent to minimizing the energy of the renormalized Hamiltonian,

$$H_{GA} = \sum_{i,j,\sigma} g_{ij}^\sigma t_{ij} c_{i\sigma}^\dagger c_{j\sigma} + \sum_{i,\sigma} \varepsilon_{i\sigma} (c_{i\sigma}^\dagger c_{i\sigma} - n_{i\sigma}), \quad (3)$$

where the Gutzwiller renormalization factor,

$$g_{ij}^\sigma = \frac{\langle \Psi | c_{i\sigma}^\dagger c_{j\sigma} | \Psi \rangle}{\langle \Psi_0 | c_{i\sigma}^\dagger c_{j\sigma} | \Psi_0 \rangle} \simeq \sqrt{\frac{x_i x_j}{(1 - n_{i\sigma})(1 - n_{j\sigma})}}, \quad (4)$$

and $\varepsilon_{i\sigma}$ is determined by $\partial \langle H_{GA} \rangle / \partial n_{i\sigma} = 0$,

$$\varepsilon_{i\sigma} = \frac{1}{2(1 - n_{i\sigma})} \sum_j g_{ij}^\sigma t_{ij} \langle c_{i\sigma}^\dagger c_{j\sigma} + h.c. \rangle - \varepsilon_{i0}. \quad (5)$$

Physically, $\varepsilon_{i\sigma}$ is the local kinetic energy per doped spin- σ electron measured relative to the average over both spins, $\varepsilon_{i0} = -\sum_\sigma (1 - n_{i\sigma}) \varepsilon_{i\sigma}$.

In the uniform phase, $n_{i\sigma} = n_\sigma$, $g_{ij}^\sigma = g^\sigma$, $\varepsilon_{i\sigma} = \varepsilon_\sigma$,

$$\varepsilon_\sigma = \frac{1}{(1 - n_\sigma)} \sum_k E_{k\sigma} f(E_{k\sigma} + \varepsilon_\sigma - \mu) - \varepsilon_0, \quad (6)$$

where f is the Fermi function and $E_{k\sigma} = g^\sigma [2t_1 (\cos k_y + 2 \cos \frac{\sqrt{3}k_x}{2} \cos \frac{k_y}{2}) + 2t_2 (\cos \sqrt{3}k_x + 2 \cos \frac{\sqrt{3}k_x}{2} \cos \frac{3k_y}{2}) + 2t_3 (\cos 2k_y + 2 \cos \sqrt{3}k_x \cos k_y)]$ is the renormalized quasiparticle dispersion. The quasiparticle band and the DOS in the PM phase are shown in Fig. 1a at $x = 0.3$. The bandwidth reduction is due to the Gutzwiller reduction factor $g^\sigma < 1$. The peak in the DOS near the band top is a property of the cobaltate a_{1g} band captured with up to third n.n. hopping.

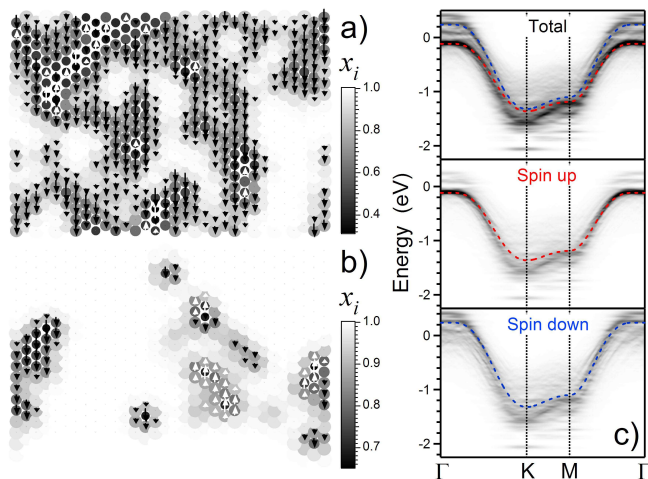


FIG. 2: (Color online) The spin (black and white arrows) and charge (local doping x_i) distribution in a typical Na(1) and Na(2) realization at $x = 0.8$ (a) and $x = 0.97$. (c) The one-particle spectral intensity (top) and its spin resolved components at $x = 0.8$.

To drive a renormalized Stoner theory for the instability of the PM phase against uniform FM order, we calculate the uniform magnetic susceptibility $\chi = \partial M / \partial h$, where $M = (n_\uparrow - n_\downarrow)\mu_B$ is the magnetization due to an infinitesimal external magnetic field h . Including the leading h -dependence of ε_σ in Eq. (6) we obtain

$$\chi = \frac{\chi_0}{1 - KN_F}, \quad K = -\frac{2}{1+x} (E_{k_F} + \varepsilon + \varepsilon_0), \quad (7)$$

where N_F is the renormalized DOS and K measures the energy per electron at the Fermi level. The latter plays the role of the effective interaction strength, replacing the Hubbard- U in the Stoner susceptibility. Fig. 1b shows the doping dependence of χ which diverges at $x_c \simeq 0.67$, corresponding to the renormalized Stoner criterion $KN_F = 1$, beyond which FM order develops at $T = 0$. The self-consistently determined magnetization shown in Fig. 1c indicates a sharp transition into the fully polarized FM, half-metallic state. The presence of the DOS peak near the band top is important for the emergence of the in-plane FM order. For example, with only nearest neighbor hopping, the FM order is completely suppressed by strong correlation [7]. We obtained the same results from the three-band Hubbard model of the t_{2g} complex. The finding of the fully polarized FM state at large x is consistent with the large FM moment of about $0.13\mu_B$ per Co site at $x = 0.82$ observed by neutron scattering [4] where $0.18\mu_B$ corresponds to a fully polarized FM state.

Now we turn to the spatially unrestricted solutions of Eqs. (3-6) and study the effects of the Na dopants. It is known that Na orders at $x = 0.5$ into $\sqrt{3} \times 2$ superstructure [28], which has been shown [23] to play an important role in alleviating geometrical frustration for the emergence of the 2×2 AF ordered state observed

by neutron scattering [25]. For $x \neq 0.5$, Na ions are disordered, and occupy randomly the preferred Na(1) and Na(2) sites directly above/below the Co or the middle of the Co triangle respectively, with a ratio of 1 : 7 at $x = 0.8$ [28]. The electrostatic potential is described by adding to the Hamiltonian (1),

$$H_V = V \sum_{i>j} \frac{\hat{n}_i \hat{n}_j}{|\vec{r}_i - \vec{r}_j|} + V_d \sum_i \sum_{\ell=1}^{N_{Na}} \frac{\hat{n}_i}{\sqrt{|\vec{r}_i - \vec{r}_\ell|^2 + d_z^2}}, \quad (8)$$

where V_d is the dopant potential strength, $d_z \simeq a$ the set-back distance of Na to the Co plane, and V the long-range Coulomb interaction that must be included to account for carrier screening. Figs. 2a and 2b show the typical charge and spin distribution of the inhomogeneous FM state at $x = 0.8$ and $x = 0.97$ on triangular lattices of 32×20 sites, with $V = 0.2\text{eV}$ and $V_d = 0.6\text{eV}$. Note that at such strength of (V, V_d) , the ordered Na at $x = 0.5$ only induces a weak charge modulation [23]. In contrast, the random distribution of Na at $x = 0.8$ leads to large fluctuations in the local electrostatic potential, causing the localization of the electrons and the formation of the non-magnetic Co^{3+} clusters where $x_i \simeq 1$. This result is in line with NMR: the presence of Co^{3+} for $x > 0.65$ but not at $x = 0.5$ [22, 29]. The one-particle spectral intensity in Fig. 2c clearly demonstrates the coexistence of localized and itinerant band-like states. Interestingly, AF correlated regions emerge at $x = 0.8$ in locally underdoped regions in Fig. 2a. In these regions, x is much smaller and the kinetic AF correlation imbedded in the Gutzwiller factor in Eq. (3) prevails due to the alleviated AF frustration by charge inhomogeneity, as proposed for the “0.5 phase” [23]. As a result, the average magnetic moment in Fig. 2a is reduced from the fully polarized value to about $0.13\mu_B$ per Co site, in qualitative agreement with the finding of neutron scattering [4]. For stronger potential fluctuations, FM clusters with AF domain walls emerge, as seen more prominently at $x = 0.97$ in Fig. 2b. These glassy behaviors arise because the localized states formed out of the majority spin band are pushed above E_F and occupied by holes, as shown in the spin-resolved spectral intensity in Figs. 2c.

To further study the localized magnetism, we consider the limit $x = 1$ and ask what happens when a few holes are doped into the band insulating NaCoO_2 by the Na vacancy. The hidden correlation effects are brought out by the slightest amount of doping. Fig. 3a displays the case of a single hole added by a Na(2) vacancy. Instead of adding the hole into the minority of the spin-polarized bands, localized states are created and pinned near the Fermi level (Fig. 3a) to accommodate the doped hole, leading to the formation of the spin-1/2 local moment distributed near the Na vacancy as shown in Fig. 3b for Na(1) and Na(2) respectively. The localized states induced by the Na electrostatic potential [21] are spin-split by $\Delta_i = \varepsilon_{i\uparrow} - \varepsilon_{i\downarrow} = (1/2x_i) \sum_j g_{ij}^\dagger (t_{ij} c_{i\uparrow}^\dagger c_{j\uparrow} + h.c.)$.

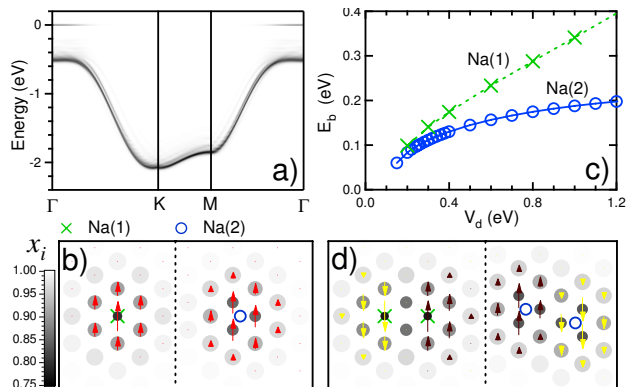


FIG. 3: (Color online) (a) Spectral intensity of one-hole doped by a Na(2) vacancy at $V_d = 1.0\text{eV}$. (b) Spin and charge distribution of the $S=1/2$ local moment near a Na(1) and a Na(2) vacancy. (c) The local moment “binding energy” E_b as a function of V_d induced by a Na(1) or Na(2) vacancy at $V_d = 0.6\text{eV}$. (d) Spin/charge distribution around two Na(1) and two Na(2) vacancies showing AF correlations between the local moments.

The latter has a localized profile whose amplitude $E_b = \Delta_{\max} - \Delta_{\min}$ is used as a measure of the binding energy of the local moment. In Fig. 3c, E_b is plotted as a function of the bare Na potential V_d . The local moment develops ($E_b > 0$) for V_d as small as 0.2eV . Because the Na(1) vacancy is directly above a Co site, E_b is enhanced, making it easier for the local moment to form near Na(1) vacancies. For even smaller V_d , it becomes difficult for our finite size numerical calculations to discern the localized states and the values of E_b , leaving open the possibility of self-trapped, spontaneous local moment formation without the Na potential.

When the Na vacancies are isolated, the spin-1/2 local moments behave as free moments, contributing to significant spin entropy in the Na-rich part of the phase diagram. As the vacancy density increases, i.e. as the average x reduces, the local moments begin to overlap and their interactions become important. We find that nearby local moments have AF correlations. As shown in Fig. 3d, since the AF frustration is alleviated by the associated charge inhomogeneity, two Na(2) or Na(1) vacancies induce two AF correlated local moments with zero net magnetization. As the local density of Na vacancy increases, FM clusters develop which eventually evolve into the macroscopic FM state. Our findings provide a complimentary description of the evolution from local magnetic clusters to macroscopic FM state observed by recent μSR experiments [5] and interpreted in terms of a change in the Co^{3+} spin state that involves the higher Co-3d e_g orbitals [10, 32].

We conclude with a discussion of an outstanding puzzle in the ARPES experiments. A large hole-like FS is observed at $x = 0.8$ with a volume much larger than what is expected by the Luttinger counting in a PM state [30, 31]. A natural explanation is that this corresponds to the minority spin band of the itinerant half-metallic state with

in-plane FM order. Such an interpretation, although in line with that of the neutron scattering experiments [4], implies a filled majority band below the Fermi level which has yet to be detected by ARPES. Our study suggests another possible scenario where the in-plane FM order associated with the 3D A-type AF order does not develop on the 2D surface at finite temperatures. The larger than expected FS comes instead from the loss of the doped electrons due to Na-induced localization and are “taken out” of the t_{2g} bands. For example, a substantial fraction of the doped electrons on the surface can be localized to form the nonmagnetic Co^{3+} similar to Fig. 2a. This picture is appealing given the recent finding by NMR of valence disproportionation associated with significant Co^{3+} formation for $0.65 < x < 0.75$ [22]. Interestingly, the same picture within the present theory suggests that in the extremely sodium rich phases $x > 0.96$, it is the localization of a fraction of holes near the Na vacancies that gives rise to the local magnetic clusters observed by μSR experiments [5]. Further studies are clearly needed to better understand the coexistence of itinerant and localized magnetism in the sodium rich cobaltates.

We thank H. Ding and P. A. Lee for many useful discussions. This work is supported by DOE grant DE-FG02-99ER45747.

-
- [1] K. Takada, H. Sakurai, E. Takayama-Muromachi, F. Izumi, R.A. Dilanian, T. Sasaki, *Nature (London)* **422**, 53 (2003).
 - [2] M.L. Foo, Y. Wang, S. Watauchi, H.W. Zandbergen, T. He, R.J. Cava, N.P. Ong, *Phys. Rev. Lett.* **92**, 247001 (2004).
 - [3] A.T. Boothroyd, R. Coldea, D.A. Tennant, D. Prabhakaran, L.M. Helme, C.D. Frost, *Phys. Rev. Lett.* **92**, 197201 (2004).
 - [4] S.P. Bayrakci, I. Mirebeau, P. Bourges, Y. Sidis, M. Enderle, J. Mesot, D.P. Chen, C.T. Lin, B. Keimer, *Phys. Rev. Lett.* **94**, 157205 (2005).
 - [5] C. Bernhard, Ch. Niedermayer, A. Drew, G. Khaliullin, S. Bayrakci, J. Strempler, R.K. Kremer, D.P. Chen, C.T. Lin, B. Keimer, *EPL* **80**, 27005 (2007).
 - [6] M. Lee, L. Viciu, L. Li, Y. Wang, M.L. Foo, S. Watauchi, R.A. Pascal Jr., R.J. Cava, N.P. Ong, *Nature Materials*, **5**, 537 (2006).
 - [7] J. Merino, B.J. Powell, R.H. McKenzie, *Phys. Rev.* **B73**, 235107 (2006).
 - [8] J.O. Haerter, M.R. Peterson, B.S. Shastry, *Phys. Rev. Lett.* **97**, 226402 (2006).
 - [9] M. M. Korshunov, I. Eremin, A. Shorikov, V.I. Anisimov, M. Renner, W. Brenig, *Phys. Rev.* **B75**, 094511 (2007).
 - [10] M. Daghofer, P. Horsch, G. Khaliullin, *Phys. Rev. Lett.* **96**, 216404 (2006).
 - [11] S. Zhou, M. Gao, H. Ding, P.A. Lee, Z. Wang, *Phys. Rev. Lett.* **94**, 206401 (2005).
 - [12] H. Ishida, M.D. Johannes, and A. Liebsch, *Phys. Rev. Lett.* **94**, 196401 (2005).
 - [13] C.A. Marianetti, K. Haule, O. Parcollet,

- cond-mat/0612606.
- [14] A. Bourgeois, A.A. Aligia, T. Kroll, M.D. Nunez-Regueiro, Phys. Rev. B **75**, 174518 (2007).
- [15] D.J. Singh, Phys. Rev. B **61**, 13397 (2000).
- [16] M.Z. Hasan, Y.-D. Chuang, D. Qian, Y.W. Li, Y. Kong, A. Kuprin, A.V. Fedorov, R. Kimmmerling, E. Rotenberg, K. Rossnagel, Z. Hussain, H. Koh, N.S. Rogado, M.L. Foo, R.J. Cava, Phys. Rev. Lett. **92**, 246402 (2004).
- [17] H.B. Yang, S.-C. Wang, A.K.P. Sekharan, H. Matsui, S. Souma, T. Sato, T. Takahashi, T. Takeuchi, J.C. Campuzano, R. Jin, B.C. Sales, D. Mandrus, Z. Wang, H. Ding, Phys. Rev. Lett. **92**, 246403 (2004).
- [18] H.B. Yang, Z.-H. Pan, A.K.P. Sekharan, T. Sato, S. Souma, T. Takahashi, R. Jin, B.C. Sales, D. Mandrus, A.V. Fedorov, Z. Wang, H. Ding, Phys. Rev. Lett. **95**, 146401 (2005).
- [19] D. Qian, L. Wray, D. Hsieh, L. Viciu, R.J. Cava, J.L. Luo, D. Wu, N.L. Wang, M.Z. Hasan, Phys. Rev. Lett. **97**, 186405 (2006).
- [20] P. Zhang, W. Luo, M.L. Cohen, S.G. Louie, Phys. Rev. Lett. **93**, 236402 (2004).
- [21] C.A. Marianetti and G. Kotliar, Phys. Rev. Lett. **98**, 176405 (2007).
- [22] I.R. Mukhamedshin, H. Alloul, G. Collin, N. Blanchard, cond-mat/0703561.
- [23] S. Zhou and Z. Wang, Phys. Rev. Lett. **98**, 226402 (2007).
- [24] O.I. Motrunich and P.A. Lee, Phys. Rev. B **69**, 214516 (2004).
- [25] G. Gasparovic, R.A. Ott, J.-H. Cho, F.C. Chou, Y. Chu, J.W. Lynn, Y.S. Lee, Phys. Rev. Lett. **96**, 046403 (2006).
- [26] G. Kotliar and A.E. Ruckenstein, Phys. Rev. Lett. **57**, 1362 (1986).
- [27] J.O. Haerter and B.S. Shastry, Phys. Rev. Lett. **95**, 087202 (2005).
- [28] H.W. Zandbergen, M. Foo, Q. Xu, V. Kumar, R.J. Cava, Phys. Rev. B **70**, 024101 (2004); Q. Huang, M.L. Foo, R.A. Pascal Jr., J.W. Lynn, B.H. Toby, T. He, H.W. Zandbergen, R.J. Cava, Phys. Rev. B **70**, 184110 (2004).
- [29] J. Bobroff, G. Lang, H. Alloul, N. Blanchard, G. Collin, Phys. Rev. Lett. **96**, 107201 (2006).
- [30] D. Qian, D. Hsieh, L. Wray, Y.-D. Chuang, A. Fedorove, D. Wu, J.L. Luo, N.L. Wang, L. Viciu, R.J. Cava, M.Z. Hasan, Phys. Rev. Lett. **96**, 216405 (2006).
- [31] H. Ding, et. al. to be published.
- [32] C. Bernhard, A.V. Boris, N.N. Kovaleva, G. Khaliullin, A.V. Pimenov, L. Yu, D.P. Chen, C.T. Lin, B. Keimer, Phys. Rev. Lett. **93**, 167003 (2004).